

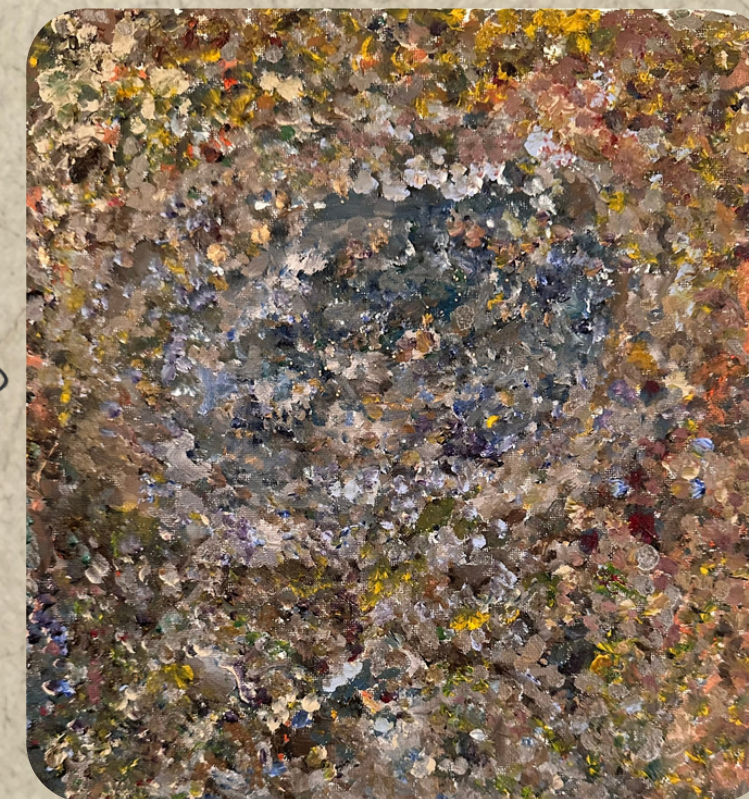
Golden Enterprises Solutions Inc.



Parchment, Writing, Ancient...



History, Manifolds,
Surjective Submersions,
Topology...



Analogue... Digital...

$$\begin{aligned} & \text{Legend: } \sin(K(x)) \xrightarrow{\quad} K(\sin(x)) \\ & \sin(x) \xrightarrow{x} \sin(x) \\ & \sin(x) \xrightarrow{x^2} \sin(x^2) \\ & \sin(x) \xrightarrow{x^3} \sin(x^3) \\ & \sin(x) \xrightarrow{x^4} \sin(x^4) \\ & \sin(x) \xrightarrow{x^5} \sin(x^5) \\ & \sin(x) \xrightarrow{x^6} \sin(x^6) \\ & \sin(x) \xrightarrow{x^7} \sin(x^7) \\ & \sin(x) \xrightarrow{x^8} \sin(x^8) \\ & \sin(x) \xrightarrow{x^9} \sin(x^9) \\ & \sin(x) \xrightarrow{x^{10}} \sin(x^{10}) \\ & \sin(x) \xrightarrow{x^{11}} \sin(x^{11}) \\ & \sin(x) \xrightarrow{x^{12}} \sin(x^{12}) \\ & \sin(x) \xrightarrow{x^{13}} \sin(x^{13}) \\ & \sin(x) \xrightarrow{x^{14}} \sin(x^{14}) \\ & \sin(x) \xrightarrow{x^{15}} \sin(x^{15}) \\ & \sin(x) \xrightarrow{x^{16}} \sin(x^{16}) \\ & \sin(x) \xrightarrow{x^{17}} \sin(x^{17}) \\ & \sin(x) \xrightarrow{x^{18}} \sin(x^{18}) \\ & \sin(x) \xrightarrow{x^{19}} \sin(x^{19}) \\ & \sin(x) \xrightarrow{x^{20}} \sin(x^{20}) \end{aligned}$$

Truth
Nature
Peace

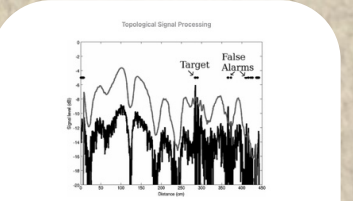
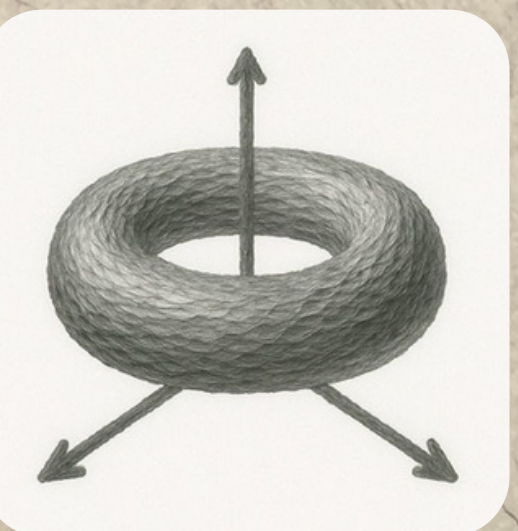


Fig. 2.14 Thresholding a sensor signal (blue) using the detection threshold (gray) to result in detections (black dots)
An example of the CFAR process. Fig. 2.14 shows sensor echoes collected by the author in which a reflective target was located at a range of 200 cm from the sensor. The input signal is shown in blue, and represents acoustic signal strength as a function of time. The detection threshold is shown in gray, and represents a signal taken as a global section of σ . The signal was collected using an acoustic horn antenna and digitized by a laptop sound card at a sampling rate of 44.1 kHz. Blocks of 100 adjacent samples (containing the target) were used to calculate a local average. A fixed detection threshold, which included an offset of 6 dB, the resulting threshold is shown in gray on Fig. 2.14. The detection threshold is shown in gray. The detection threshold has a large dot at the “0 dB” level, and correspond to the places where the global section of σ takes the value 1. The target echo is clearly visible, but the signal exceeded the threshold at other locations as well. These other locations are called false alarms and are probably due to other reflectors existing in the scene.

Remark 2.6
The component maps π_m can be “tuned” considerably to reduce false alarms. For instance, some implementations construct a detection threshold of the form

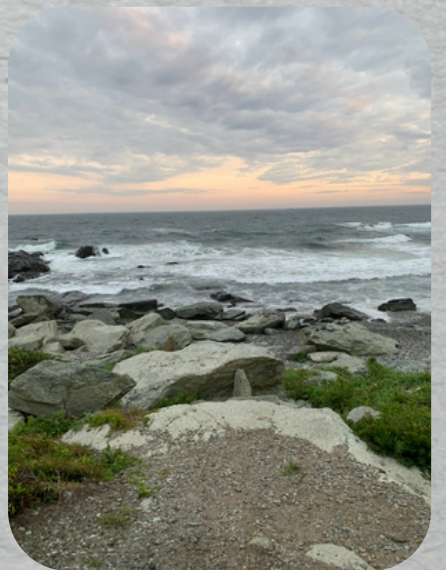
$$\frac{1}{|W|^2-N} \sum_{m=1}^{|W|^2-N} \pi_m^{-1} M - N - |W|^2 \sum_{m=1}^{|W|^2-N} \pi_m + 2\pi_m$$

which rounds binning the threshold with potentially noninteger values. Other implementations weight the terms in the above sum. The interested reader is encouraged to consult Stimson (1998) for details about practical CFAR implementations.



Golden Enterprises Solutions Inc.

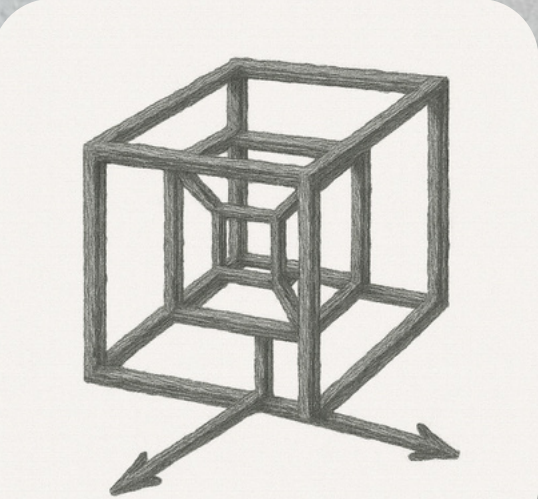
Eclipse, ellipse, sun swept
dune beneath the moon...



Transcendence



Smooth, Natural



Elucidation



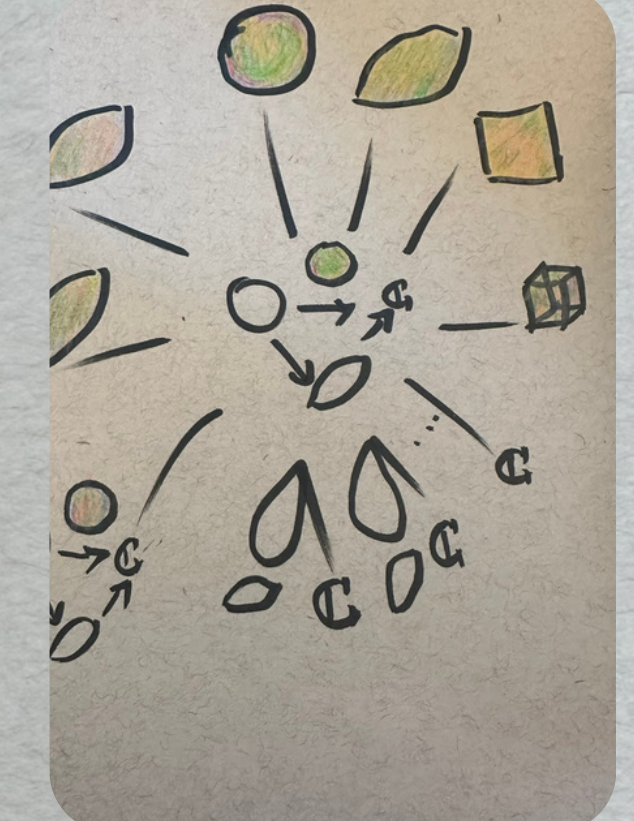
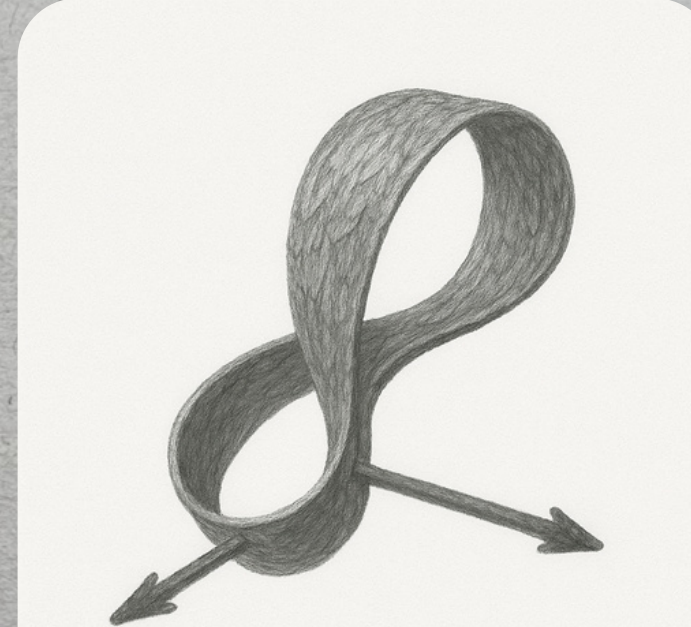
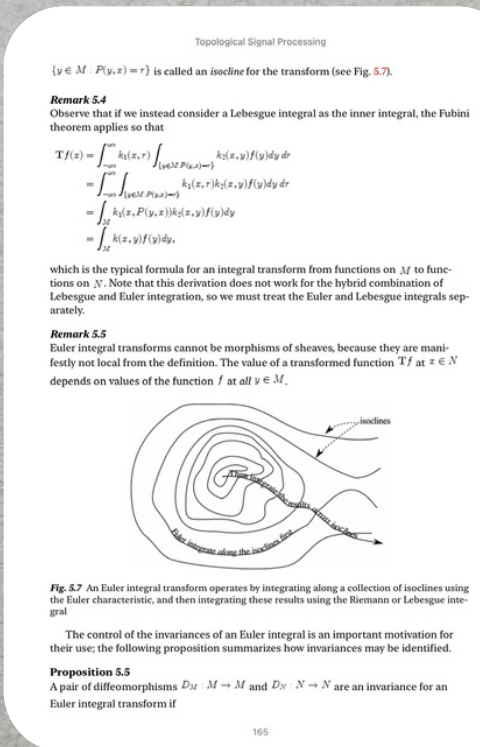
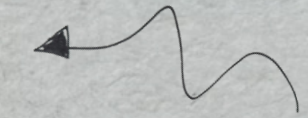
Truth, Science



Serenity



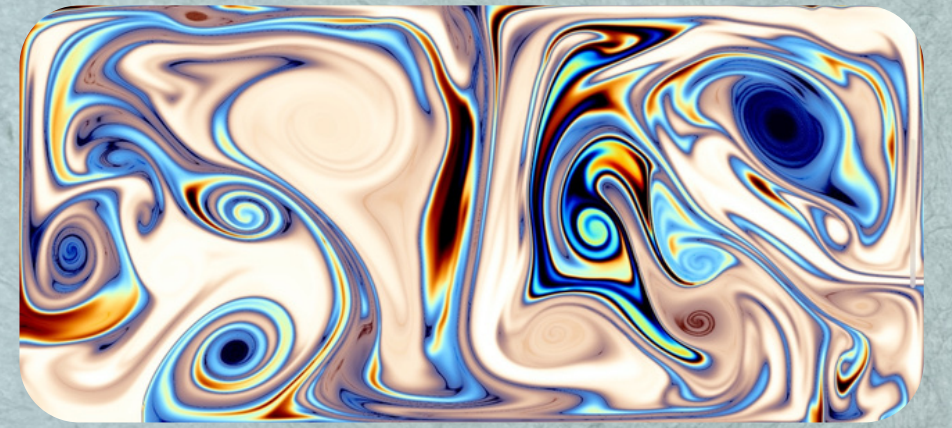
Meditation



Golden Enterprises Solutions Inc.



Cultural
Immersion, Data
Analysis, New
Life!



Inversion...
Complete...
1, 1, 2, 3, 5, Phi,
x, y, z, blue,
yellow

Mind, Body,
Spirit



SpaceTime Study

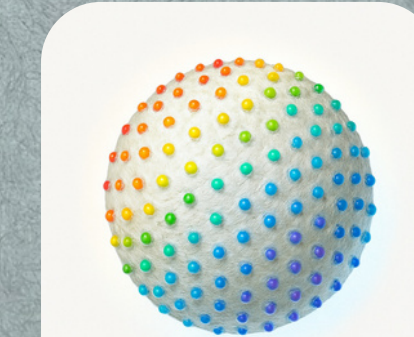
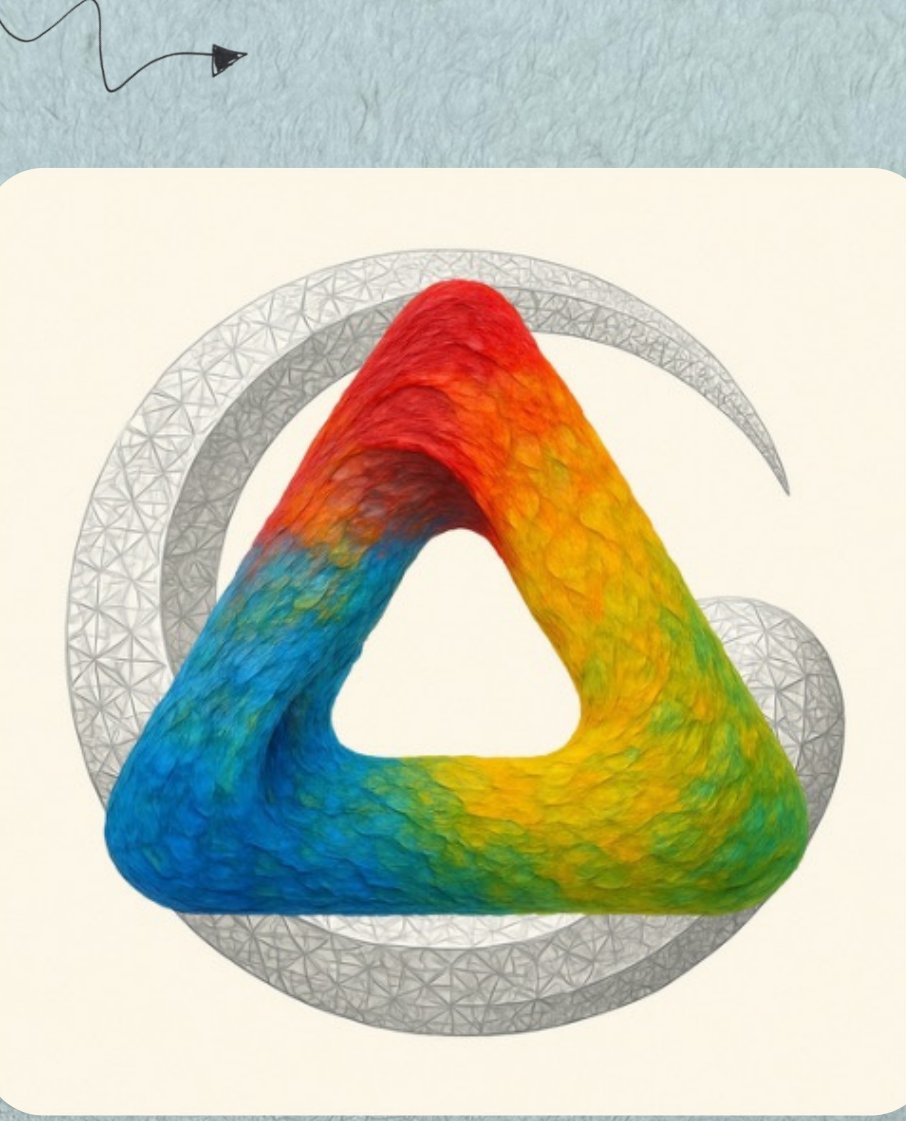
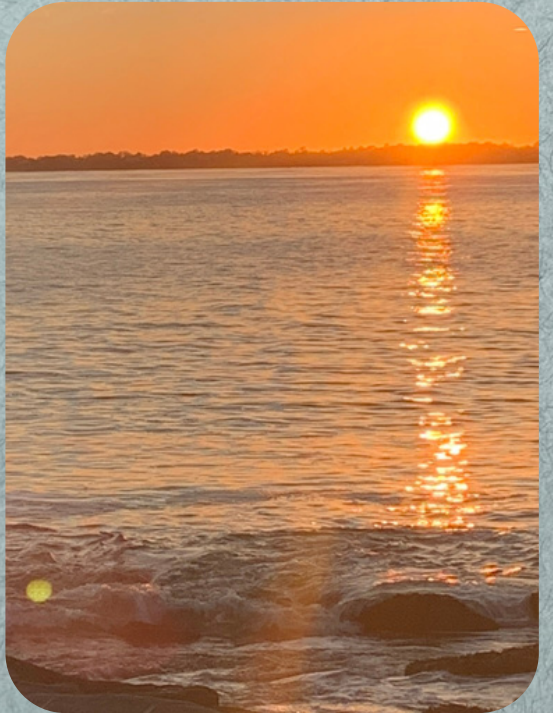
- Clock, pendulum, gravity driven, mechanical
- Clock subjective submersion
- Escape subjective submersion

$$T = 2\pi \sqrt{\frac{L}{g}}$$

now, adj, vb
now, adj, vb
now, adj

natural, functor, function,

\square injection, surjection, bijection. Δ



Transformations,
Representations,
Sheaves



Topological Signal Processing

The following calculation due to Baryshnikov and Ghrist (2009) shows how to recover the number of elements of $v = \{U_1, \dots\}$ from h (see Fig. 5.4). It is useful to think of h as the sum of indicator functions

$$h(x) = \sum_i 1_{U_i}$$

Suppose that $U_i \in v$, then

$$\int h \, d\chi = \int \sum_i 1_{U_i} \, d\chi = \sum_i \int 1_{U_i} \, d\chi = \sum_i \chi(U_i) = |v| \chi(U_i)$$

Provided $\chi(U_i) \neq 0$, then

$$|v| = \frac{1}{\chi(U_i)} \int h \, d\chi \quad (5.3)$$

The interpretation of this calculation is somewhat striking. Suppose that there is a finite collection of large targets that are visible to a dense field of sensors spread over a region X . If each sensor returns an anonymous count of the targets visible to it, this calculation shows how to recover the total number of targets from these counts.

Fig. 5.5 Values of the function h in which four target support sets overlap

Example 5.8

Consider the function h shown in Fig. 5.5, which arises from the collection of four contractible target support sets. (Since each target support is an open set, this function is lower semicontinuous; the value along each boundary is the lower of the two neighboring values.) Tabulating the values of the function according to the dimension of the cells, we have

Accumulating these values, the Euler integral is $3 \times 2 + 2 \times (-1) = 4$, which is the number of target support sets.

Table



Golden Enterprises Solutions Inc.



Gold, Iridescence, Griggio,
Yah ah Tay, Language....



$$T = 2\pi \sqrt{\frac{L}{g}}$$

Handwritten notes on the left side of the equation:

- $T = \text{period}$
- $V = \text{Voltage}$
- $I = \text{Current}$
- $P = \text{Power}$
- $R = \text{Resistance}$
- $L = \text{inductance}$
- $m = \text{mass}$
- $\theta = \text{angle}$
- $F = \text{Force}$
- $a = \text{acceleration}$
- $t = \text{time}$
- $g = \text{gravity}$

Biological Signal Processing

The following calculation due to Berryman and Ghosh (2009) shows how to recover the number of elements in $\Omega_1 \cup \dots \cup \Omega_n$ from δ_i (see Fig. 3.3). It is useful to think of δ_i as the sum of indicator functions

$$\delta_i(A) = \sum_{j \in A} \delta_j$$

Suppose that $\delta_i \neq 0$, i.e.,

$$\int_A \delta_i = \int_A \sum_{j \in A} \delta_j = \sum_{j \in A} \int_A \delta_j = \sum_j \delta_j(A) = \sum_j \psi_j(\Omega_j) = \psi_j(\Omega_i)$$

Provided $\psi(\Omega_i) \neq 0$, then

$$\int_A \delta_i = \int_A \psi_j(\Omega_i) = \psi_j(A)$$

The interpretation of this calculation is somewhat striking. Suppose that there is a number of targets (e.g., birds) whose supports are visible in the form of sets Ω_i over a region X . If one records an average count of the counts of the targets visible in the calculation shows how to recover the total number of targets from these counts.

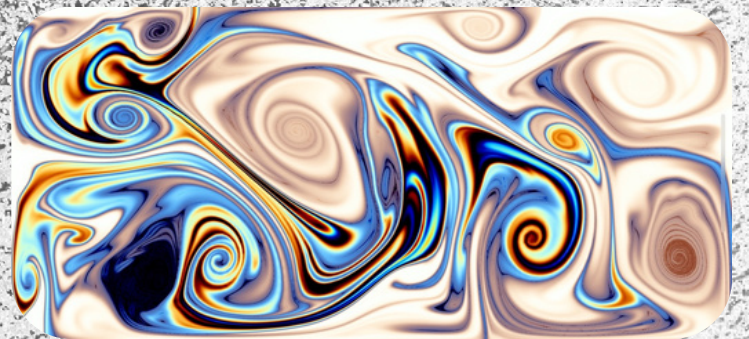
Fig. 3.3 Values of the function ψ_j in which four target support sets overlap

Example 3.8 Consider the function ψ shown in Fig. 3.3, which arises from the collection of four non-overlapping target support sets. Since each target support is an open set, this function is lower semicontinuous. Calculating the values of the function according to the dimension of the cells, we get

Integrating these values, the Euler integral is $3 + 2 + 2 + (-1) = 4$, which is the number of target support sets.



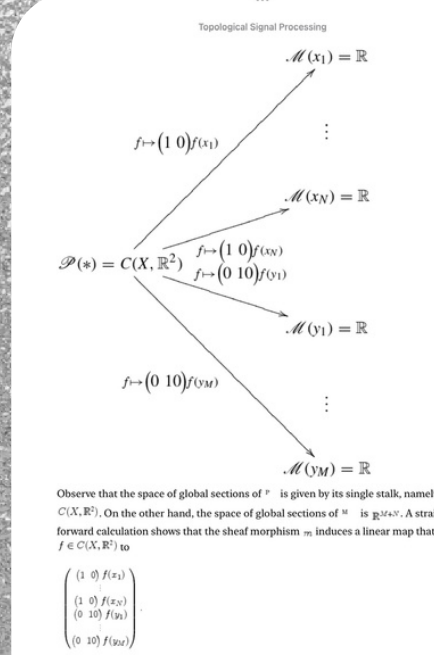
Golden Enterprises Solutions Inc.



Day... Night...
Cold... Warm



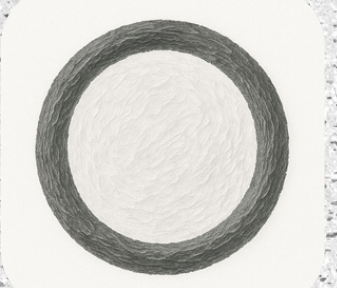
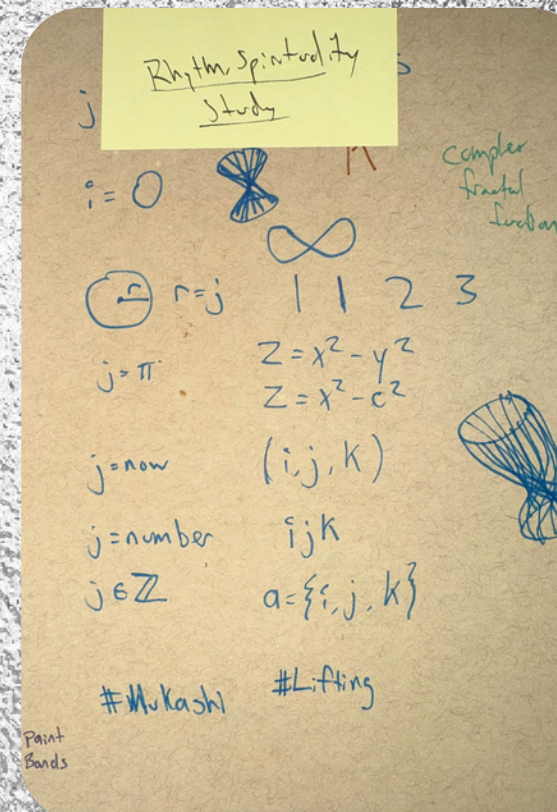
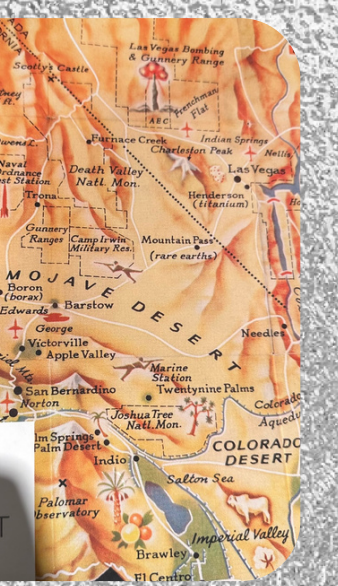
Square, Circle,
Trieste



Time,
Space,
Energy



Earth, Land,
Hand, Rhythm



Golden Enterprises Solutions Inc.



Play,
Learn,
Swirl,
Curl

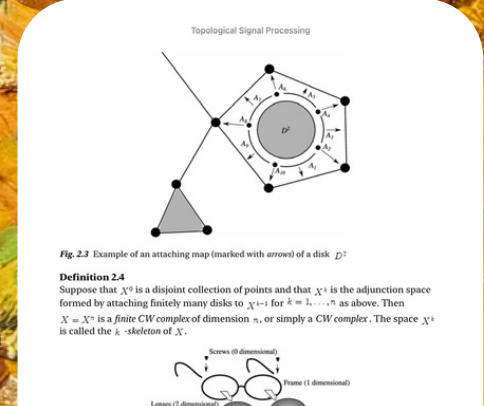


Fig. 2.3 Example of an attaching map (marked with arrows) of a disk D^2

Definition 2.4
Suppose that X is a discrete collection of points and that X^{k-1} is the adjunction space formed by attaching finitely many disks to X^{k-1} for $k = 1, \dots, n$ as above. Then $X = X^n$ is a finite CW complex of dimension n , or simply a CW complex. The space X^n is called the k -skeleton of X .



Fig. 2.4 An attachment construction is like an exploded view for a topological space

Attachment constructions like these are powerful tools for understanding how a space is assembled from its parts. They play a similar role to exploded view diagrams (see Fig. 2.4) in assemblies. Because of this graphical connection, attachment constructions can be visualized with an attachment diagram, showing how the cells are attached, such as in Fig. 2.5. Each cell is shown and the links represent attachments (drawn from low-dimensional cells to higher-dimensional cells). Usually, we suppress any attachments that are compositions of other attachments.

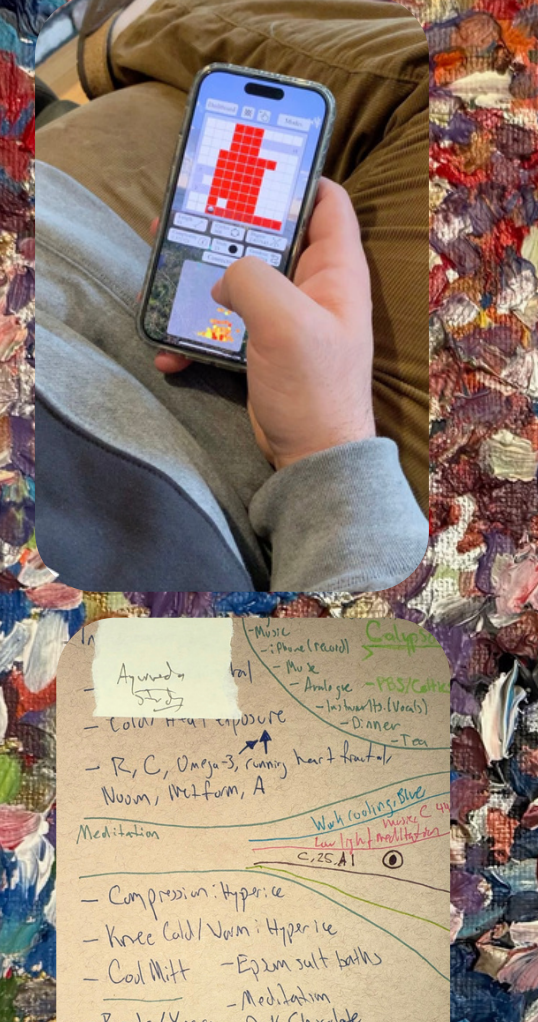
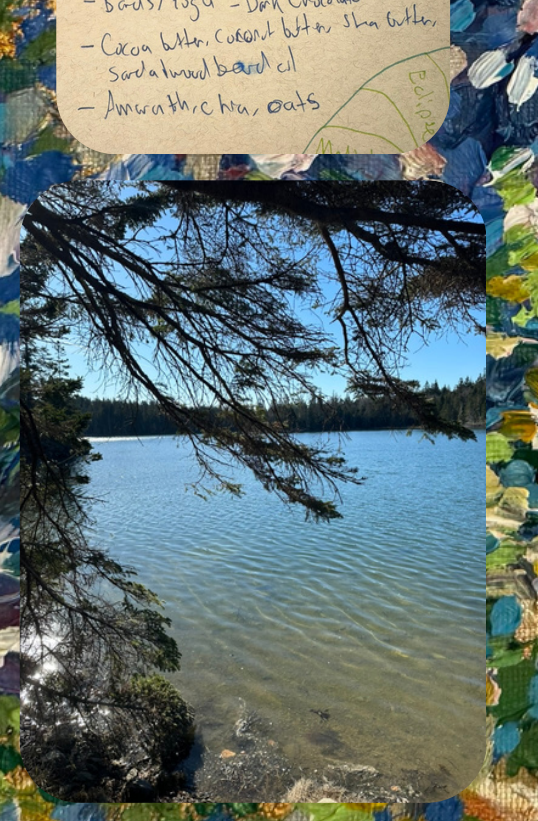
Remark 2.1
The attachment diagram of an attachment construction is a set that is partially ordered by the sequence of attachments. When we exhibit an attachment diagrams, we display its Hasse diagram.

25

Deep, Ocean,
Mist, Crisp,
Abyss



Home...
Letting Go...



Calming
- Music
- Phone (read)
- Music
- Analogs
- Instruments (Vocals)
- Dancer
- Nourish, Metform, A
With breathing, Blue
Lavender, Meditation
C.25.41

- Compression: Hyperice
- Knee Cold/Warm: Hyperice
- Cool Mitt - Epsom salt baths
- Meditation
- Bands/Yoga - Dark Chocolate
- Cocoa Butter, Coconut butter, Shea Butter, Sardine/avocado oil
- Amaranth, chia, oats
M.1
P.10/10